Available online at www.sciencedirect.com
SCIENCE DIRECT®
Nuclear Instruments and Methods in Physics Research A 540 (2005) 295–304
NUCLEAR INSTRUMENTS & METHODS IN PHYSICS RESEARCH Section A
www.elsevier.com/locate/nima

Detection of single electrons by means of a Micromegas-covered MediPix2 pixel CMOS readout circuit

M. Campbell[a], M. Chefdeville[b], P. Colas[b], A.P. Colijn[c], A. Fornaini[c,d], Y. Giomataris[b], H. van der Graaf[c], E.H.M. Heijne[a], P. Kluit[c], X. Llopart[a], J. Schmitz[d], J. Timmermans[c,*], J.L. Visschers[c]

[a]*CERN/MediPix Consortium, Geneva, Switzerland*
[b]*DAPNIA, CEA Saclay, 91191 Gif sur Yvette Cedex, France*
[c]*NIKHEF, PO Box 41882, #1009 DB Amsterdam, The Netherlands*
[d]*University of Twente/MESA, The Netherlands*

Received 2 September 2004; received in revised form 17 November 2004; accepted 19 November 2004
Available online 25 December 2004

Abstract

A small drift chamber was read out by means of a MediPix2 readout chip as a direct anode. A Micromegas foil was placed 50 μm above the chip, and electron multiplication occurred in the gap. With a He/isobutane 80/20 mixture, gas multiplication factors up to tens of thousands were achieved, resulting in an efficiency for detecting single electrons of better than 90%. We recorded many frames containing 2D images with tracks from cosmic muons. Along these tracks, electron clusters were observed, as well as δ-rays.

Keywords: Micromegas; MediPix2; TPC; Single electron; Pixel; Pixel segmented anode

1. Introduction

Recently [1] we have demonstrated the possibility to read out a drift chamber by means of a direct, pixel segmented active anode. Images of the interaction of ^{55}Fe quanta with the gas were obtained (see Fig. 1) with a rather low gas amplification factor, since these quanta create some 220 primary electrons in a small volume of argon gas. The aim of the research presented in this paper is to prove the feasibility of the detection of single (drifting) electrons, based on the same pixel sensor/Micromegas combination.

Our goal is to develop a single-electron sensitive monolithic device *TimePixGrid* consisting of a CMOS pixel matrix *TimePix* covered with a Micromegas [2]. Each pixel will be equipped with a preamp, a discriminator, a threshold DAC

*Corresponding author. Tel.: +31 20 5925112; fax: +31 20 5925155.
E-mail address: timmermans@nikhef.nl (J. Timmermans).

0168-9002/$ - see front matter © 2004 Elsevier B.V. All rights reserved.
doi:10.1016/j.nima.2004.11.036

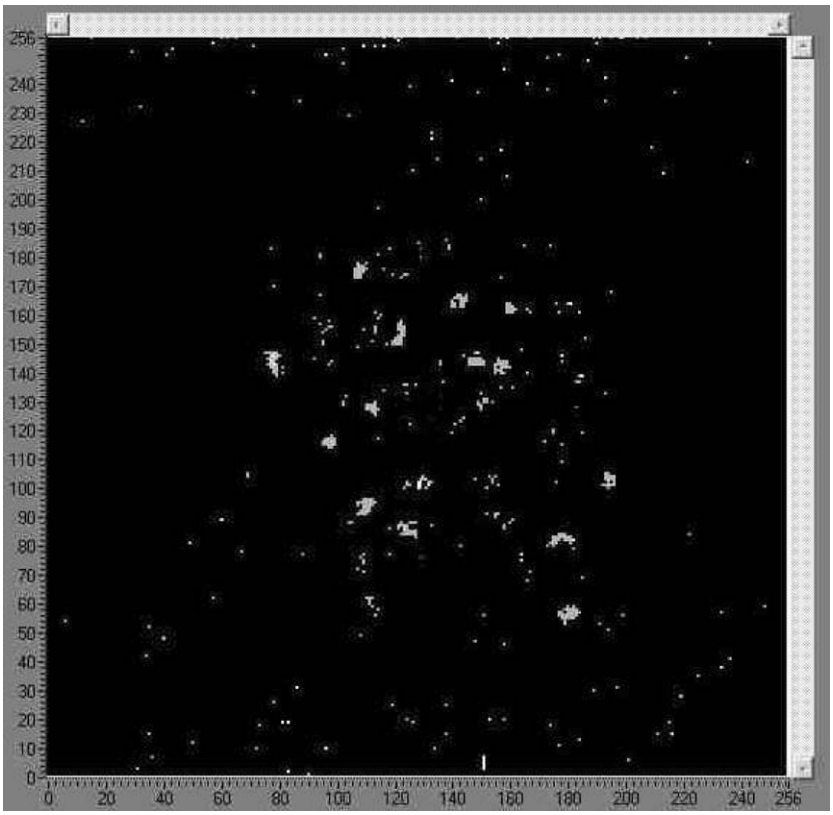

Fig. 1. Image acquired with the Medipix2/Micromegas prototype TPC [1].

and time stamp circuitry. Such a sensor would replace the wires (or GEMs, or Micromegas), anode pads, feedthroughs, readout electronics and cables of TPCs and could generally be applied in gaseous (drift) chambers. We intend to integrate the Micromegas grid onto the *TimePix* chip by means of wafer post-processing technology (*In-Grid*).

In Section 2 the test chamber including the MediPix2 readout chip and the Micromegas are described. In Section 3 details on single-electron detection and signal development are presented. Section 4 describes the data readout and the analysis of the cosmic ray tracks. It includes a discussion on the observation of so-called Moiré patterns in the detected hit pixel distribution. The paper ends with conclusions on the present work and an outlook to our future plans.

2. The chamber, MediPix2 and Micromegas

2.1. The chamber

The test chamber is depicted in Fig. 2. Above an aluminium base plate, a cathode foil is fixed, by means of spacers, forming a drift gap of 15 mm height. By means of a cut-out in the base plate, the MediPix2 chip (mounted on a brass pedestal) is placed flush with the base plate upper plane. On top of the chip, a Micromegas foil, fixed on a frame, is held in position by means of two silicon rubber strings (see Fig. 3).

2.2. The MediPix2 CMOS pixel sensor

A MediPix2 chip [3–5] was applied as an experimental readout device. This CMOS chip

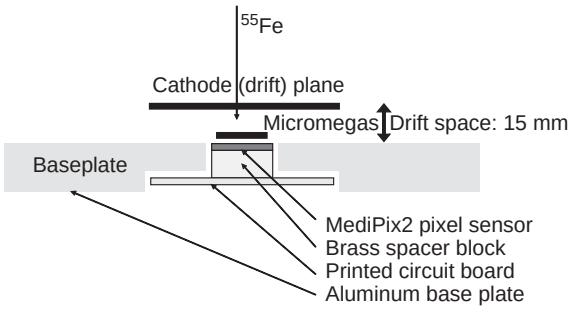

Fig. 2. Layout of the chamber with the MediPix2, the Micromegas and the drift gap.

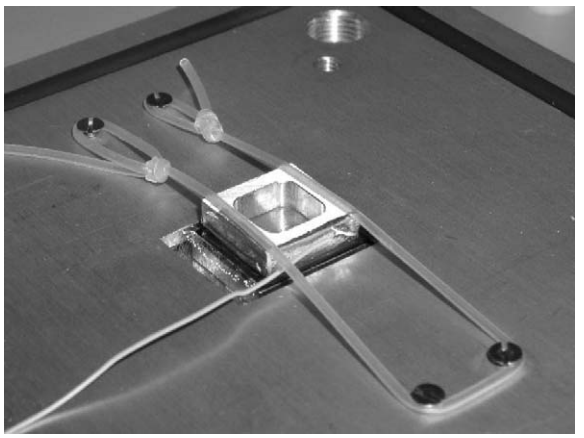

Fig. 3. Mounting of the Micromegas onto the MediPix2 sensor.

contains a square matrix of 256×256 pixels, each with dimensions $55 \times 55\,\mu m^2$. Each pixel is equipped with a low-noise preamp, discriminator, threshold DACs, a 14-bit counter and communication logic. One edge of the chip has aluminium bonding pads. The outer dimensions of the chip are $16.12 \times 14.11\,mm^2$. The MediPix2 chip has been designed for X-ray imaging applications. For that particular application, an X-ray semiconductor converter (i.e. Si or CdZnTe), in the form of a corresponding pixel matrix, is mounted onto the MediPix2 chip by means of bump bonding. The assembly of a MediPix2 chip and an X-ray converter forms a complete X-ray imaging device. For each pixel the number of absorbed X-ray quanta in a given acquisition time is counted, and the combined pixel content forms the X-ray image. In our application we use the "naked" MediPix2 chip, without an X-ray convertor.

Originally, each pixel of the MediPix2 chip is covered for a large part with an insulating passivation layer; the conductive pad (octagonally shaped, 25 μm wide) is large enough to accommodate a bump bond sphere. The electric field in the gap between the MediPix2 and the Micromegas is in the order of 7 kV/mm, and discharges were expected when some 70% of the anode surface is covered with an insulating material.

In order to prevent these discharges, the MediPix2 wafers were post-processed by MESA + [6]. The post-processing consisted of a deposition of a thin aluminium layer using lift-off lithography. This allows deposition of metal on the anode matrix without modification of the bond pads. The pixel pads were thus enlarged to reach a metal coverage of 80% of the anode plane (see Fig. 4). Electrical tests showed that the preamplifier functionality was unaffected by this post-processing. We have applied both the modified and the non-modified versions of the MediPix2 chip.

2.3. The Micromegas

The Micromegas is a copper foil, thickness 5 μm, with holes of 35 μm diameter in a square pattern with 60 μm pitch [7]. At the foil side facing the MediPix2 chip, poly-imide pillars (height 50 μm, diameter 80–140 μm, pitch (square) 840 μm) are attached. The Micromegas, in its frame, was held on the MediPix2 chip by means of two silicon rubber strings. When the voltage on the Micromegas was applied (200–500 V), the electrostatic force pulls the mesh towards the chip, and the insulating pillars define the proper gap size.

In order to prevent HV breakdowns, a square kapton foil, with a square hole of $10.5 \times 10.5\,mm^2$, was placed between the Micromegas and the MediPix2. The chamber was placed such that the drift direction was vertical. The fiducial drift volume of $10.5 \times 10.5 \times 15\,mm^3$ is hit by a cosmic ray particle about once per minute [8].

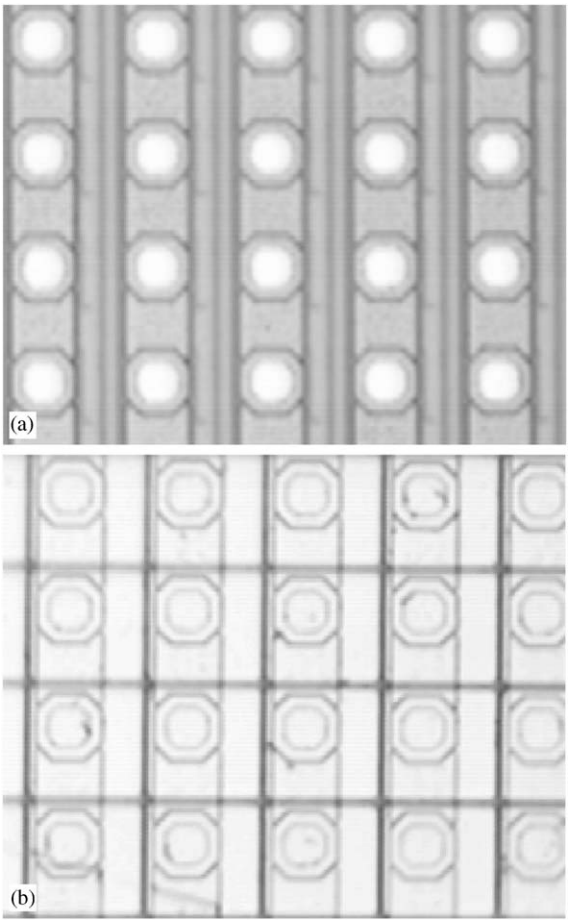

Fig. 4. The Medipix2 chip before (a) and after (b) the *wafer post-processing*. The original pad (Al, $25 \times 25\,\mu m$) is covered with an aluminium pad of $45 \times 45\,\mu m$. Note that no Micromegas mesh has yet been mounted on the chips shown in this figure.

3. Single-electron detection; signal development

A muon, originating from a cosmic shower, traversing the drift volume, will create clusters of electrons along its track. The cluster density, and the distribution of the number of electrons per cluster depends on the gas composition, gas density and the muon momentum. If argon is the main component of the gas (at atmospheric pressure), some 3 clusters per millimetre are created for a minimum ionising muon, and the average number of electrons per cluster is 2.5 [9]. Consequently, on average some 7 primary electrons are created per track length of 1 mm. The mean distance between two primary electrons, projected onto the anode plane, is much larger than the pixel pitch, and therefore typically single electrons will enter a Micromegas hole. For this reason the single-electron response is essential for the performance of the pixel-segmented anode readout. The counting of primary ionisation clusters would allow a precise measurement of the energy loss dE/dx [10].

After an electron has entered a hole, it will be multiplied, and the number of electrons grows exponentially towards the anode pads. The centre of gravity of the points of electron–ion separations is positioned at $D \ln 2/\ln M$ away from the anode, where D is the distance between the Micromegas and the anode and M is the gas multiplication factor. With $D = 50\,\mu m$ and $M = 3000$ the charge centre of gravity is about $4\,\mu m$ away from the anode. The electrons will all arrive within 1 ns at the anode. Most of the ions, moving much slower, arrive within 30–50 ns at the Micromegas, depending on the gas composition and pressure. If a point charge crosses the avalanche gap, then the potentials of both the Micromegas and the anode change linearly with the distance of the point charge to the anode plane. The charge on the anode pad below the avalanche is the sum of the negative electron charge and the positive induced ion charge. The fast component has an amplitude of 10% of the total charge. The latter (slow) component decreases during the drift of the ions towards the Micromegas. On adjacent pads, however, the same ions will induce a positive charge, which will be at a maximum when the ions are halfway (after some 25 ns) between the anode and the Micromegas. This charge is only a fraction of the avalanche charge, and is back to zero after the arrival of the ions at the Micromegas. On these pads we may thus expect a bipolar current signal.

The peaking time constant of the MediPix2 preamp/shaper is 150 ns. This is large with respect to time constants of the signal development. The preamp/shaper output is therefore proportional to the avalanche charge, and the discriminator threshold can be expressed unambiguously in the number of electrons appearing at the input pad.

Although the design value of the input noise equivalent of the pixel preamps was 90 electrons, the thresholds were set at 3000 electrons in order to limit background hits due to (digital) feedback noise, possibly caused by the 4 mm long bonding wires.

The average of the number of electrons in an avalanche, initiated by a single electron is the gas multiplication factor M [9]. The fluctuations in the number of electrons in an avalanche follow an exponential function [11]:

$$p(n) = \frac{1}{M} e^{-n/M},$$

where $p(n)$ equals the probability to have an avalanche with n electrons in total. The avalanche distribution is shown for several values of the gain M in Fig. 5. Since the preamp noise is small with respect to the threshold, and since there is no electron attachment, we apply the simple exponential distribution instead of approaches like the Polya distributions [12] which include several 2nd-order effects.

With a threshold set at T electrons, avalanches smaller than that are not detected. The efficiency ε to detect single electrons is then given by

$$\varepsilon = e^{-T/M}.$$

If, for instance, the threshold is set to a value that equals the gain, the efficiency equals $1/e = 0.37$. In Fig. 6 the efficiency curve is depicted as a function of the gain M for a threshold $T = 3000$.

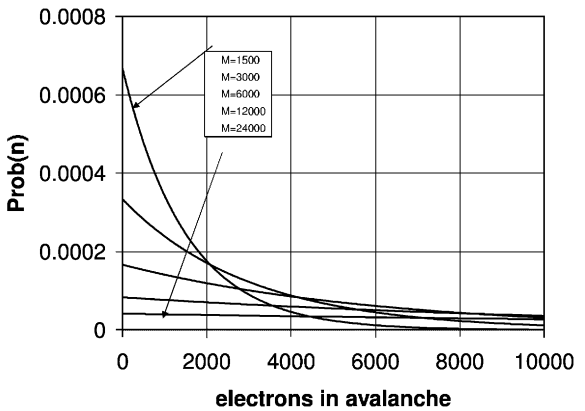

Fig. 5. Probability distribution for the number of electrons in an avalanche for several values of the gas gain M.

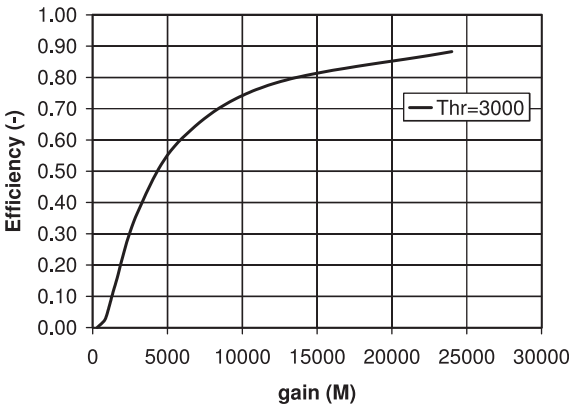

Fig. 6. Single-electron detection efficiency as a function of the gas gain for a threshold set at 3000 e^-.

We would like to keep the gas gain as low as possible in order to (a) limit the risk of discharges and ageing and (b) limit the ion space charge. With the present MediPix2, with its lowest threshold of 3000 electrons, a gain of 10 k would correspond to a single-electron efficiency of 0.74. For this reason we used He mixtures which allow a high gain, with a small risk of discharges.

Due to discharges, four MediPix2 chips were destroyed within 24 h of operation. The MediPix2 chip has no protection circuitry at its pixel input pads other than the source and drain diffusions of the transistors responsible for leakage current compensation. We noticed some damage of the pixel pads, probably due to a high temperature in the discharge region. For *InGrid*, we intend to eliminate discharge damage by (a) covering the bottom of the Micromegas with a (high) resistive layer, limiting the participating charge, (b) covering the anode pads with a (high) resistive layer, in combination with (c) a protective network, for each pixel, connected to the anode pad.

4. Results

4.1. Cosmic ray tracks and data readout; calibration

The MediPix2 sensor can be externally enabled and stopped, followed by a readout sequence in

which the pixel counter data is transferred to a computer. We enabled the counters during an exposure time of 15 or 60 s, followed by recording the image frame in the form of 65k counter contents. No trigger was applied.

The (positive) charge signals on the Micromegas were read out by means of a low-noise charge sensitive preamp, with a decay time constant of 1 μs. Signals from a ^{55}Fe source could be recorded, and the preamp was calibrated with charge signals from a block wave, injected by means of a 10 pF capacitor. Together with the known number of primary electrons per ^{55}Fe quantum, the gas amplification can be measured.

With a He/isobutane 80/20 mixture, we observed signals from ^{55}Fe events with −390 V on the Micromegas and −1000 V on the drift cathode plane. This is expected given the large density of primary electrons in the interaction point [1] and the gain at this voltage of about 1k. We then increased the voltage on the Micromegas to −470 V, corresponding to a gain of approximately 19k. With a threshold setting of 3000 e^-, we expect a single-electron efficiency of 0.85, and cosmic rays were observed.

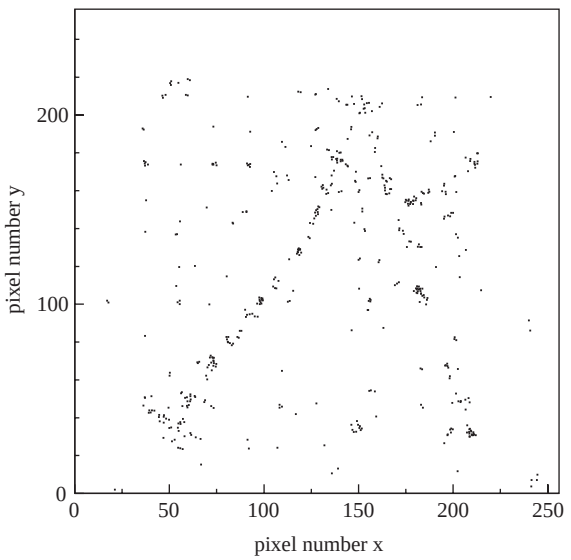

Fig. 7. Image recorded from the MediPix2/Micromegas prototype TPC showing cosmic charged particle tracks together with some background. All the hit pixels during an acquisition time of 15 s are shown.

Some typical events are shown in Figs. 7–9. Fig. 7 shows a cosmic event with environmental background. Fig. 8 shows a cosmic muon that knocks out a delta electron. Fig. 9 shows a selected

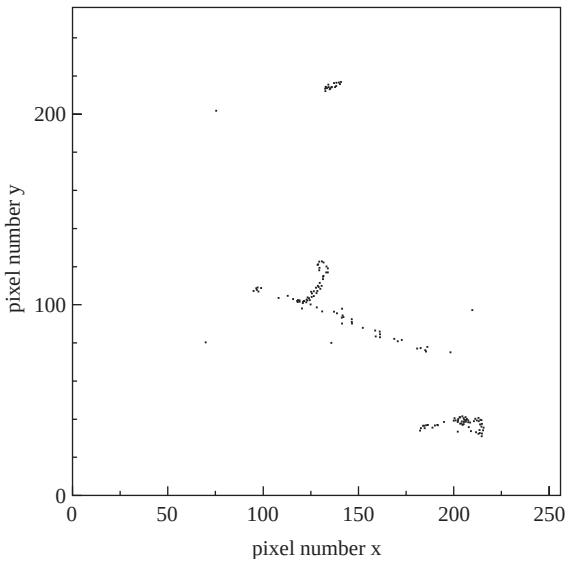

Fig. 8. Image recorded from the MediPix2/Micromegas prototype TPC showing a cosmic charged particle track together with a δ-electron.

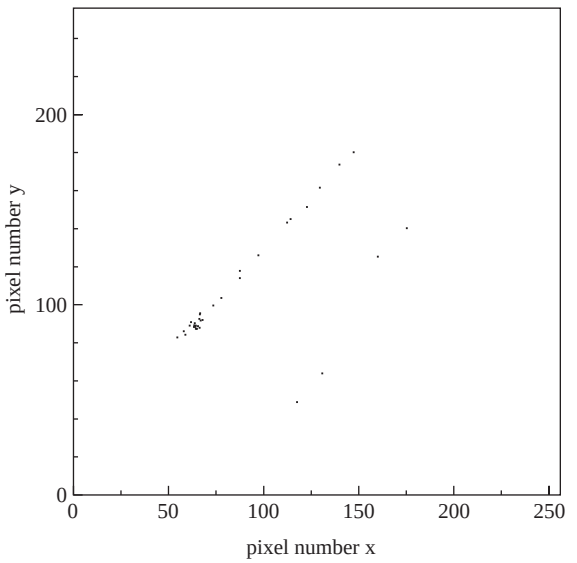

Fig. 9. Image recorded from the MediPix2/Micromegas prototype TPC showing selected cosmic charged particle tracks. The selections and noise filtering are described in the text.

cosmic muon. The selection cuts are described below. In this event the effect of diffusion can be observed in the spread of the hits along the track.

A selection to obtain a sample of clean cosmic events was made. For the data a map of the noisy pixels was made. The signal from the edges and the inefficient upper left corner of the detector were removed. First, a straight line was searched using a Hough transform. Pixels within a distance of 20 pixels are associated to the track. The following quantities were calculated: the number of associated pixels, the r.m.s. of the distance to the track, the track length in the detector plane L_d (in millimetres). The full 3D track length L (in millimetre) is estimated as $L = \sqrt{L_d^2 + 15^2}$. The track is split into two equal parts and the minimum r.m.s. value of the two parts is calculated. Clusters are formed by stepping along the track and grouping all hits within a distance of 5 pixels. The number of clusters is counted.

The following criteria were applied to select an event:

- the number of associated pixels larger than 5 and the fraction of associated pixels to the track to the total number of pixels hit larger than 80%;
- L_d larger than 2.75 mm (i.e. 50 pixels);
- the r.m.s. less than 4;
- the number of associated pixels per millimetre of 3D track length should be less than 4.

In total, 164 events were selected in the data. The distributions of some physical quantities are shown in Fig. 10.

A simulation programme was written generating cosmic minimum ionising particles with an angular distribution $\propto \cos^2\theta$. The muon was tracked through the sensitive volume of the detector. Clusters were generated with an average of 1.4 per millimetre and per cluster 3.16 electrons were generated using a Poissonian distribution [13]. The electrons were drifted toward the MediPix2 detector with a diffusion constant of 220 μm per square root centimetre. Inefficient zones of the MediPix2 detector in the region between the pixels and below the pillars were put in. The detector is assumed to have an efficiency of 100% in the efficient zones. Note that multiple hits on a single pixel are at present not separated. The same selection cuts were applied to data and simulation.

The distribution of the minimum r.m.s. is sensitive to the diffusion constant. Data give an average value of 2.0 pixels (simulation 2.4). This implies that the diffusion constant is slightly better than 220 μm per square root centimetre. The observed number of pixels hit per millimetre is 1.83 on average (2.70 simulation). The number of clusters per millimetre is 0.52 (simulation 0.60). The average 3D track length is 16.5 mm. The number of clusters per millimetre agrees within 15% with the simulation, and the number of electrons within 35%. Note that a 100% efficiency is assumed for the detector. Inefficiencies have also more impact on the number of electrons than on the number of clusters. If we take into account systematic uncertainties on the expected number of clusters and electrons per millimetre, uncertainties on the efficiency and operating conditions of the detector, we find the agreement reasonable. Later experiments will focus on a more precise quantitative understanding of the detector.

4.2. Moiré effects

Fig. 11 shows an image, obtained after irradiating the chamber with β's from a ^{90}Sr source. The top-left corner of the image is clearly less efficient. This is due to the non-flatness of the Micromegas in its frame. Apparently, the electrostatic force could not entirely eliminate the warp in the Micromegas foil. Here, the pillars are not in contact with the MediPix2 surface. The gap is wider and the gain is reduced. The dead regions due to the pillars are clearly visible as well.

Fig. 12 shows the image, taken with a non-modified MediPix2 sensor, after irradiating the drift volume with the ^{90}Sr source. Band-shaped regions with a reduced efficiency are clearly visible. Note that these bands are present in two perpendicular directions. The same effect is visible in an image (Fig. 13) which is the sum of all cosmic rays obtained during one night of data taking, again with a non-modified MediPix. The corresponding image from a modified MediPix2 is shown in

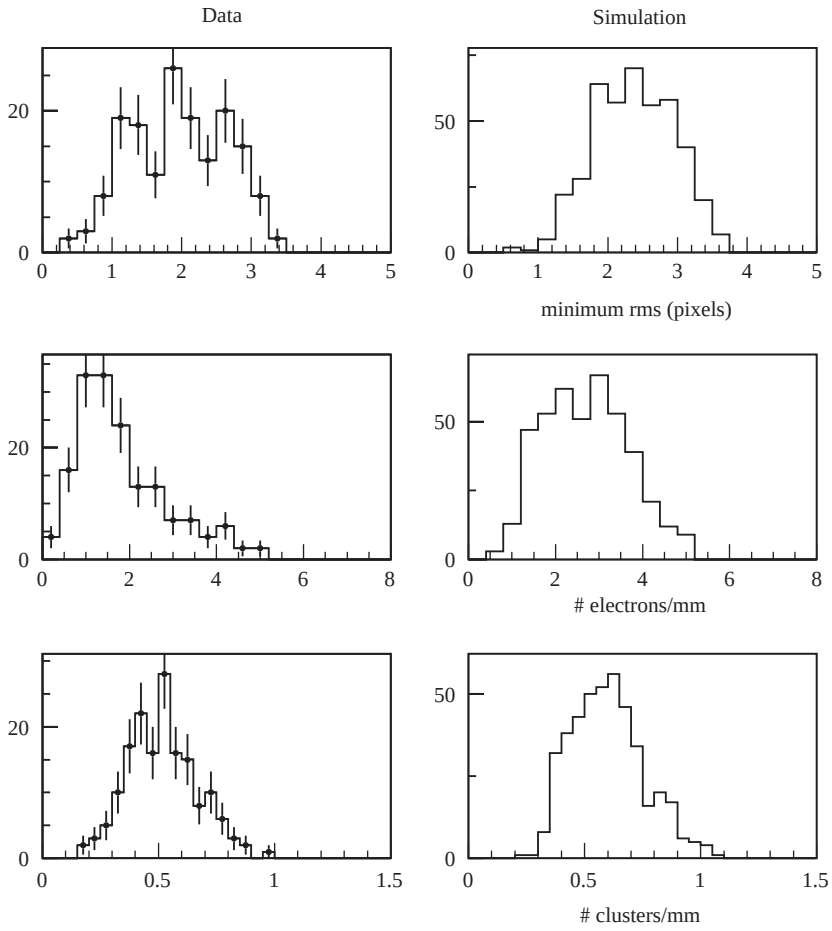

Fig. 10. Distributions of some quantities used in the analysis for selected cosmic data (left) and in the simulation (right). Top: the minimum of the two r.m.s. values for a track. Centre: the number of reconstructed electrons per millimetre of 3D track length. Bottom: the number of reconstructed primary clusters per millimetre of 3D track length.

Fig. 14, where bands are still present, but much less pronounced. The bands can well be explained in terms of a Moiré effect: the pixel size of the MediPix2 sensor ($55 \times 55\,\mu m^2$) does not match the pitch of the holes in the Micromegas ($60 \times 60\,\mu m^2$). Consequently, the hole position with respect to its nearest pixel centre, shifts when one follows a pixel row or pixel column. The relative hole position repeats after $60/(60-55) = 12$ pixels.

The Moiré effect can be understood in terms of the pixel signal amplitude being dependent on the relative position of a Micromegas hole and the pixel pad. Such a variation could not be explained by the charge sharing between 2 or 4 pixels for avalanches (with a certain width), located in the region near a pixel edge, because we did not observe the consequent effect of having significantly more clusters with 2, 3 or 4 hit pixels in the same less efficient regions.

Instead, the less efficient regions can be explained by the partly insulator-covered anode. If a Micromegas hole is located above the joint of 2 pixels, or above the 4 adjacent corners of 4 pixels, the drifting electron will be pulled towards 1 pad which is relatively far away. Along this drift path the electric field is less strong, and the gain is smaller. This effect explains the difference in the

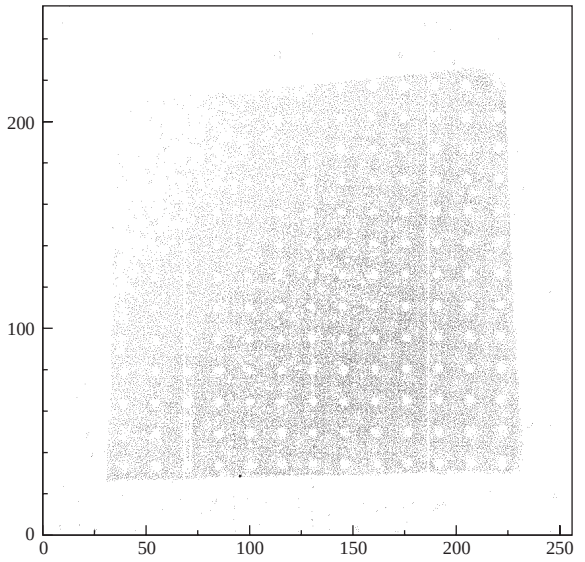

Fig. 11. Superimposed images recorded from the MediPix2/Micromegas prototype TPC after irradiation with β's from a ^{90}Sr source.

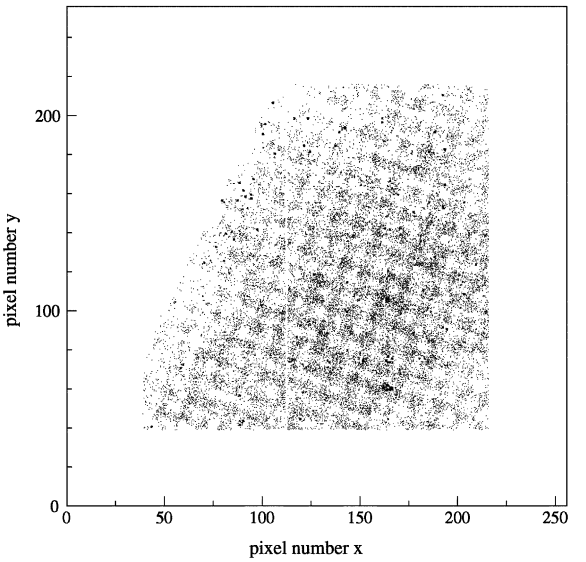

Fig. 13. Superimposed images recorded with a non-modified MediPix2 sensor during one night of cosmics data taking.

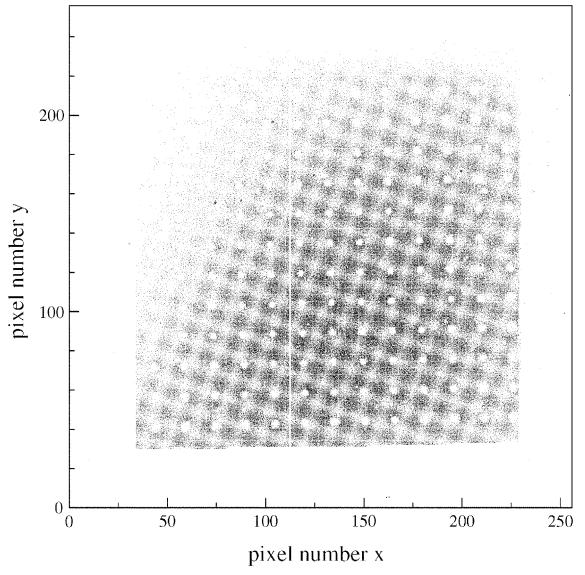

Fig. 12. Superimposed images recorded with a non-modified MediPix2 sensor after irradiation with β's from a ^{90}Sr source.

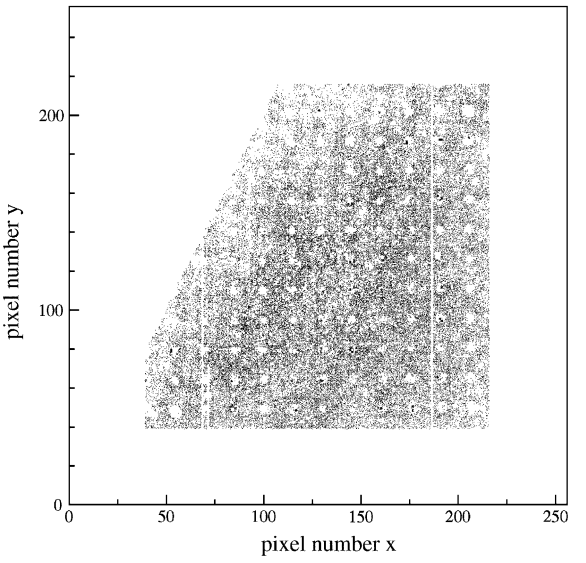

Fig. 14. Superimposed images recorded with a modified MediPix2 sensor during one night of cosmics data taking.

amplitudes of the Moiré effect when using modified or non-modified MediPix2 sensors.

The probability for 2-fold clusters was found to be homogeneous, and not subject to the Moiré effect, but the measured value was found to be significantly higher than the Monte Carlo simulation (30% and 10%, respectively). We explain this by the occurrence of very large but not rare

avalanche charges, following the distribution shown in Fig. 5. A neighbouring pixel can be hit due to capacitive crosstalk, in spite of the (positive) induced charge.

5. Conclusions and outlook

We have demonstrated that single electrons can be detected with an assembly of a CMOS pixel chip and a Micromegas foil, with an efficiency larger than 0.9, in a He-based gas mixture. Bubble chamber-like images of cosmic ray tracks have been obtained and even δ-electrons could be observed. The device allowed one to reconstruct the number of primary ionisation clusters per unit of track length, giving the possibility of a measurement of the ionisation loss $\mathrm{d}E/\mathrm{d}x$.

For the future *TimePixGrid*, the grid holes are precisely centred above the pixel pads, eliminating the non-homogeneity of the efficiency. The fact that the non-modified MediPix could stand the strong electric field, together with its strong Moiré effect, makes us confident that we can apply a pixel circuit with small pads, provided that the grid holes are well centred above the pads. The pad capacity can be kept small, simplifying the pixel input circuit. The inter-pad capacity is then also small, reducing the crosstalk between neighbouring pixels. A very small pad may reduce the maximum radiation dose, due to ageing, and an optimum must be found.

The combination of a pixel sensor and a Micromegas offers an instrument capable of giving a full 2D image of all single electrons in a gaseous volume. By replacing the MediPix2 sensor with a *TimePix* chip, a full 3D image is expected to be within reach. These circuits will open new possibilities for particle detection, in terms of position resolution, track separation and energy loss measurements. As another example, the polarisation of X-ray quanta can be measured [14], after its interaction with gas, from the direction of the photo-electron, which is registered accurately with the new device. Applied with a thin drift space of 1 mm, the device could be used as a fast vertex detector in high radiation environments.

Acknowledgements

We thank the MediPix Collaboration for providing us with several wafers with MediPix2 chips, for the readout software and hardware. We would like to thank Arnaud Giganon, Wim Gotink, Joop Rövekamp and Tom Aarnink for their creative and essential contributions to the realisation of the test detectors.

References

[1] P. Colas, A.P. Colijn, A. Fornaini, Y. Giomataris, H. van der Graaf, E.H.M Heijne, X. Llopart, J. Schmitz, J. Timmermans, J.L. Visschers, Proceedings of the 10th Vienna Conference on Instrumentation, Vienna, 2004; Nucl. Instr. and Meth. A 535 (2004) 506; See also Ref. [14].
[2] Y. Giomataris, et al., Nucl. Instr. and Meth. A 376 (1996) 29.
[3] X. Llopart, M. Campbell, R. Dinapoli, D. San Segundo, E. Pernigotti, IEEE Trans. Nucl. Sci. NS-49 (2002) 2279.
[4] M. Conti, M. Maiorino, G. Mettivier, M.C. Montesi, P. Russo, IEEE Trans. Nucl Sci. NS-50 (2003) 869.
[5] D. San Segundo Bello, M. van Beuzekom, P. Jansweijer, H. Verkooijen, J.L. Visschers, Nucl. Instr. and Meth. A 509 (2003) 164.
[6] Mesa + Research Institute, University of Twente, The Netherlands.
[7] The Micromegas has been made by the CERN EST Workshop.
[8] Particle Data Group, Phys. Rev. D 66 (2002) 010001
[9] F. Sauli, Principles of operating of multiwire and proportional drift chambers, CERN Yellow Report 77-09, 1977.
[10] M. Hauschild, in: J.S. Kang, S.K. Oh (Eds.), Proceedings of the International Workshop on Linear Colliders, Jeju, Korea, 2002, pp. 464–469.
[11] H.S. Snyder, Phys. Rev. 72 (1947) 181.
[12] W. Riegler, C. Lippmann, R. Veenhof, Nucl. Instr. and Meth. A 500 (2003) 144.
[13] S. Biagi, Nucl. Instr. and Meth. A 421 (1999) 234.
[14] R. Bellazzini et al., Proceedings of the 10th Vienna Conference on Instrumentation, Vienna, 2004; Nucl. Instr. and Meth. A 535 (2004) 477.